Acta Geophysica
vol. 60, no. 1, Feb. 2012, pp. 92-118
DOI: 10.2478/s11600-011-0035-z

Spatial Variations of Precursory Seismic Quiescence Observed in Recent Years in the Eastern Part of Turkey

Serkan ÖZTÜRK[1] and Yusuf BAYRAK[2]

[1]Gümüşhane University, Department of Geophysics, Gümüşhane, Turkey
e-mail: serkanozturk@gumushane.edu.tr (corresponding author)

[2]Karadeniz Technical University,
Department of Geophysics, Trabzon, Turkey
e-mail: bayrak@ktu.edu.tr

Abstract

A statistical analysis is made for the eastern part of Turkey in the beginning of 2009 by studying the phenomenon of seismic quiescence as a potential precursor of the main shocks. The results produced four areas having seismic quiescence in the beginning of 2009. These areas are observed to be centered at 39.96°N-40.69°E (around Aşkale, Erzurum), 39.36°N-39.74°E (around Ovacık, Tunceli), 39.02°N-40.52°E (including Elazığ and Bingöl), and 38.45°N-42.94°E (Van Lake).

Based on the recent results showing 5 ± 1.5 years quiescence before the occurrence of an earthquake in this region, the future earthquake would be expected between 2009.5 and 2010.5. The future earthquake occurrence may reach 2012 if we consider the standard deviation of average seismic quiescence as ±1.5 years. We have found that the $M_W = 6.0$ Elazığ earthquake on 8 March 2010, followed a seismic quiescence starting about 5 years before the main shock. Thus, special interest should be given to the other regions where the seismic quiescence is observed.

Key words: eastern Turkey, precursory seismic quiescence, decluster, seismicity pattern.

1. INTRODUCTION

There are a lot of studies on the spatial and temporal phenomenon of precursory seismic quiescence. Some of these studies on the precursors of past earthquakes suggest that particular space-time seismicity patterns, including the phenomenon of precursory quiescence, can be related to the seismo-tectonic processes that lead to earthquakes. There exist different approaches to measure, map and evaluate possible episodes of seismic quiescence (*e.g.*, RTL, PI, RI, ZMAP, *etc*.). This has the disadvantage that the results reported by different authors may not be easily compared, but it has the advantage that one may gain more confidence in a pattern that is detected by different methods. Also, the uncertainties in the results may be estimated by comparison and additional insights may be gained because of intrinsic differences in the statistical characterization of anomalies (*e.g.*, Wyss and Habermann 1988a, b; Ambraseys 1989, Taylor *et al*. 1991, Wiemer and Wyss 1994, Takanami *et al*. 1996, Wyss *et al*. 1997, 2004, Huang *et al*. 2001, Rundle *et al*. 2000).

Precursory seismic quiescence is the inner part of the doughnut pattern proposed by Mogi (1969) on the basis of visual inspection of seismicity maps. Wyss and Habermann (1988a) defined the phenomenon of seismic quiescence formally. Their amended definition reads as follows: "The quiescence hypothesis assumes that some main shocks are preceded by precursory quiescence, which is a significant decrease of the mean seismicity rate (number of events of magnitude exceeding a given threshold, per unit time), as compared to the preceding declustered background rate in the same crustal volume, judged significant by some clearly defined standard (*e.g.*, Wyss and Martirosyan 1998, Console *et al*. 2000). The rate decrease takes place within part, or all of the source volume of the subsequent main shock, and it extends up to the time of the main shock, or may be separated from it by a relatively short period of increased seismicity rate. Usually, the rate decrease is larger than 40%, and takes place in all magnitude bands". Also, Wiemer and Wyss (1994) defined the precursory quiescence hypothesis in the following way: "A statistically significant decrease of the seismicity rate that occurs in a restricted segment of a seismogenic zone. The rate decrease is terminated by a main shock and the quiescent volume covers all or a major part of the source volume".

Quiescence hypothesis is based on the assumption that the seismicity rate in large and small seismogenic volumes is constant, unless a change in process takes place (Wyss and Martirosyan 1998). Major earthquakes redistribute stress locally and thus cause aftershock sequences as well as local seismic quiescence. Creep episodes or slow earthquakes on deep extensions also redistribute stress and hence cause local increases and decreases of seismicity rate. To measure quiescence, it must be documented how constant the seismicity rate is in the study area. This is done by classifying all deviations from the average rate by their significance. If it is found that the most significant or one of the most significant deviations from a constant rate occurs near a main shock, in time and space, it may be proposed that a connection exists.

Arabasz and Wyss (1996) stated that the duration of quiescence before large earthquakes is expected to be 4.5 ± 3 years, but since it seems to depend strongly on tectonic environment and perhaps on the loading rate, it is important to measure it in the case of continental collision, since no such example of seismic quiescence has been quantitatively documented yet. However, the proposal of Wyss (1997a) of quiescence before main shocks as a precursor was placed in the "undecided" category by the experts working on behalf of that same sub-commission (Wyss 1997b). Although at least 80 authors have published case histories of this phenomenon, the hypothesis of precursory seismic quiescence is not universally accepted. As a result, it is not clear yet how common this phenomenon is, what its characteristics are, and how it is best measured quantitatively.

Since seismic quiescence analysis (*e.g.*, Gentili 2010, Rudolf-Navaro *et al.* 2010, Wang *et al.* 2010, Kumazawa *et al.* 2010, Öztürk 2011) has shown significant results in detecting precursory anomalies related to crustal main shocks, in this study we aimed to provide additional information regarding to future seismic hazard of the eastern part of Turkey, by analyzing the seismic quiescence situation in the beginning of 2009 by Z-value approach. For this reason, we investigated seismic activity changes in the eastern part of Turkey, as defined by Wyss and Habermann (1988a), using the gridding method of Wiemer and Wyss (1994) and the ZMAP analysis software (Wiemer 2001). This application investigates crustal quiescence as a precursor to some strong crustal events that occurred in the eastern part of Turkey and provide us valuable information as to the validity and existence of the phenomenon.

2. DATA AND STUDY REGION

The part of the earthquake catalogue including the time from 1970 to 2006 is taken from Öztürk (2009). He developed some relationships between different magnitude scales (body wave magnitude m_b, surface wave magnitude M_S, local magnitude M_L, duration magnitude M_D) in order to prepare a homogenous earthquake catalogue from different data sets. He prepared a homogenous instrumental data catalogue between 1970 and 2006 for M_D magnitude using these relationships. For this study, we also used the KOERI catalogue for the time period between 2006 and 2009. Seismological Observatory of KOERI, which has computed the size of all earthquakes with M_D, provides the real time data with the modern on-line and dial-up seismic stations in Turkey especially after 2000. Thus, we used M_D scale for more

Table 1

Relationships between M_D and M_L scales for 24 different source regions of Turkey. The values in the parentheses show the uncertainties (from Öztürk 2009)

Region number	Earthquakes number	Calculated relationships	Correlation coefficient r
1	20	$M_D = 0.881(\pm 0.138) \times M_L + 0.596(\pm 0.286)$	0.820
2	14	$M_D = 0.919(\pm 0.023) \times M_L + 0.292(\pm 0.048)$	0.996
3	11	$M_D = 0.991(\pm 0.080) \times M_L + 0.033(\pm 0.158)$	0.966
4	24	$M_D = 0.768(\pm 0.114) \times M_L + 1.004(\pm 0.239)$	0.808
5	4	–	–
6	26	$M_D = 0.816(\pm 0.068) \times M_L + 0.825(\pm 0.147)$	0.920
7	14	$M_D = 0.812(\pm 0.112) \times M_L + 0.726(\pm 0.234)$	0.889
8	2	–	–
9	11	$M_D = 0.432(\pm 0.339) \times M_L + 2.293(\pm 0.675)$	0.359
10	23	$M_D = 0.843(\pm 0.066) \times M_L + 0.580(\pm 0.137)$	0.935
11	81	$M_D = 0.818(\pm 0.036) \times M_L + 0.586(\pm 0.075)$	0.929
12	46	$M_D = 1.277(\pm 0.209) \times M_L - 1.372(\pm 0.434)$	0.669
13	12	$M_D = 1.113(\pm 0.389) \times M_L - 0.555(\pm 0.768)$	0.636
14	28	$M_D = 0.956(\pm 0.057) \times M_L + 0.103(\pm 0.114)$	0.952
15	70	$M_D = 0.934(\pm 0.029) \times M_L + 0.163(\pm 0.062)$	0.967
16	15	$M_D = 0.446(\pm 0.146) \times M_L + 1.900(\pm 0.291)$	0.619
17	67	$M_D = 0.748(\pm 0.043) \times M_L + 0.869(\pm 0.089)$	0.903
18	12	$M_D = 0.886(\pm 0.044) \times M_L + 0.349(\pm 0.087)$	0.985
19	18	$M_D = 0.901(\pm 0.049) \times M_L + 0.268(\pm 0.100)$	0.974
20	62	$M_D = 0.939(\pm 0.068) \times M_L + 0.091(\pm 0.138)$	0.867
21	22	$M_D = 0.876(\pm 0.069) \times M_L + 0.450(\pm 0.139)$	0.939
22	17	$M_D = 0.873(\pm 0.043) \times M_L + 0.467(\pm 0.089)$	0.980
23	11	$M_D = 1.229(\pm 0.691) \times M_L - 0.707(\pm 1.382)$	0.473
24	21	$M_D = 0.743(\pm 0.099) \times M_L + 1.211(\pm 0.222)$	0.851

reliable results and we did not prefer to calculate new empirical values of different magnitude types. In recent years, KOERI generally gives M_L magnitude for the local earthquakes with missing M_D magnitudes. In the situation that M_D is unknown in KOERI catalogue for the time period between 2006 and 2009, M_D magnitudes were calculated using the M_D-M_L relationships (Table 1) from Öztürk (2009) and we obtained 2760 earthquakes for the eastern part of Turkey in this time period. The same relationships for M_D-M_L scales are also given in Bayrak *et al*. (2009).

The bounds of the region analyzed in this study are provided from Öztürk (2009). Turkey is divided into 24 different source regions (Fig. 1a) by Öztürk (2009) considering the different previous zonation studies for modeling of seismic hazard in Turkey, plotting the existing tectonic structure (Fig. 1b) with

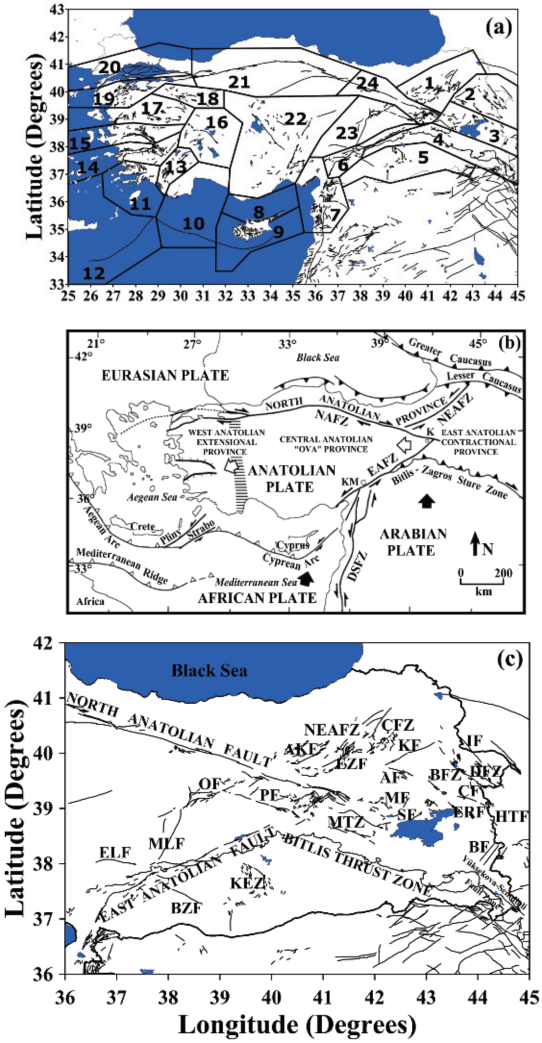

Fig. 1: (a) Seismic source zones from Öztürk (2009) together with the major tectonics; (b) Simplified tectonic map of Turkey showing major neotectonic structures and neotectonic provinces (modified from Bozkurt 2001); (c) Active fault map of the eastern part of Turkey. The major tectonic structures are modified from Şaroğlu *et al*. (1992), Bozkurt (2001), and Ulusay *et al*. (2004). Names of faults: NEAFZ – North East Anatolian Fault Zone, ÇFZ – Çobandede Fault Zone, AKF – Aşkale Fault, EZF – Erzurum Fault, KF – Kağızman Fault, AF – Ağrı Fault, IF – Iğdır Fault, DFZ – Doğubeyazıt Fault Zone, BFZ – Balıklıgölü Fault Zone, ÇF – Çaldıran Fault, ERF – Erciş Fault, HTF – Hasan-Timur Fault, BF – Başkale Fault, SF – Süphan Fault, MTZ – Malazgirt Fault, MTZ – Muş Thrust Zone, KEZ – Karacadağ Extension Zone, BZF – Bozova Fault, ELF – Elbistan Fault, MLF – Malatya Fault, OF – Ovacık Fault, PF – Pülümür Fault.

the epicenter distribution of earthquakes, and solution of focal mechanism given by TÜBİTAK Marmara Research Center for the great earthquakes occurred in Turkey between 1977 and 2002 (see also Bayrak *et al*. 2009). The eastern part of Turkey limited by the coordinates 36°N and 42°N in latitude and 36°E and 45°E in longitude is selected as an area of investigation since there are many great earthquakes occurred in this area after 2000. The major tectonic structures of the study region were adopted from different authors such as Şaroğlu *et al*. (1992), Bozkurt (2001), Ulusay *et al*. (2004) and shown in Fig. 1c (one can find all details for the relationships of M_S with the other magnitude types and all seismic zonations in Bayrak *et al*. 2009).

After the selection of the study region, the earthquake catalogue in this region is prepared. First, the earthquakes between 2006 and 2009 are selected from the whole catalogue. There are 2760 earthquakes in the time from 2006 to 2009. Also, the catalogue has 6008 earthquakes between 1970 and 2005. The final time period considered for the present work is from 17 February 1970 to 31 December 2008, and time length is about 38.87 years. The magnitudes in the used catalogue are M_D magnitude. Finally, the prepared homogeneous data catalogue for study region consisting of 8768 earthquakes (depth less than 70 km) with magnitudes greater than or equal to 1.8 during 1970-2009 is used in this study. Epicenter distributions of whole earthquakes and the principal main shocks ($M_D \geq 5.0$) in the study region are shown in Fig. 2.

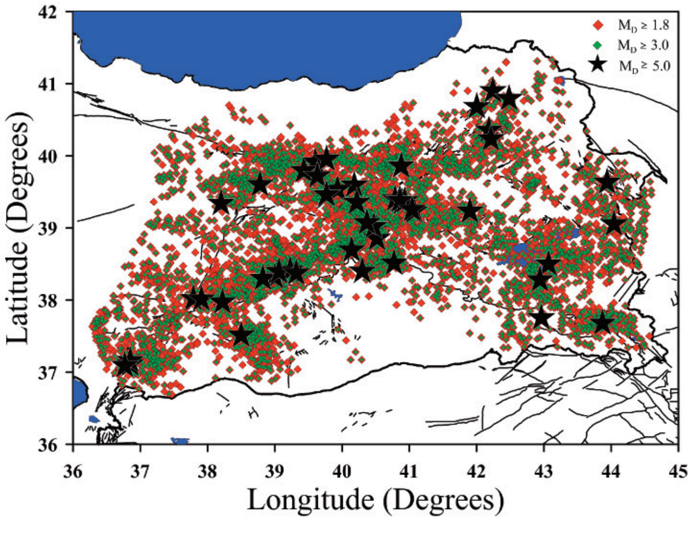

Fig. 2. Epicenter locations of earthquakes in the eastern part of Turkey with major tectonic features. All earthquakes with $M_D \geq 1.8$ and depth less than 70 km between February 1970 and December 2008 are shown. The earthquakes over the completeness threshold, $M_D \geq 3.0$, are also plotted. Stars indicate the principal main shocks with $M_D \geq 5.0$.

Table 2

Some details of earthquakes occurred in the eastern part of Turkey with magnitude $M_D \geq 5.5$ between 1970 and 2009

Date	Origin time	Long.	Lat.	Depth [km]	M_D	Region	Deaths	Damaged buildings
22 May 1971	16:43:59	40.52	38.85	3.0	5.9	Bingöl	878	9111
6 Sep. 1975	09:20:12	40.77	38.51	32.0	5.6	Diyarbakır	2385	8149
24 Nov. 1976	12:22:16	44.04	39.05	10.0	5.6	Van	3840	9232
30 Oct. 1983	04:12:28	42.18	40.35	16.0	5.8	Erzurum-Kars	1155	3241
13 Mar. 1992	17:18:39	39.63	39.72	23.0	6.5	Erzincan	653	8057
15 Mar. 1992	16:16:25	39.93	39.53	29.0	6.0	Tunceli	–	439
5 Dec. 1995	18:49:32	40.22	39.35	33.0	5.6	Tunceli	1	–
3 Dec. 1999	17:06:55	42.21	40.23	10.0	5.5	Erzurum-Kars	–	A few
27 Jan. 2003	05:06:22	39.77	39.46	5.0	6.2	Tunceli	1	50
1 May 2003	00:27:04	40.47	39.02	5.0	6.4	Bingöl	176	6000
12 Mar. 2005	07:36:08	40.85	39.38	5.0	5.6	Bingöl	–	>100
14 Mar. 2005	01:55:55	40.89	39.35	5.0	5.9	Bingöl	–	>100
21 Feb. 2007	13:05:26	39.32	38.37	5.0	5.6	Elazığ	–	A few
8 Mar. 2010	02:32:31	40.09	38.81	5.0	5.8	*Elazığ	42	–

*) This earthquake is not included in the catalogue because the analyses are made by using the earthquakes between 1970 and 2009.

Most of the seismicity catalogues are contaminated by quarry blasts. An extraordinarily high number of daytime events in a region are a likely sign of explosion activity. Polat *et al.* (2008) stated that most of the quarries have almost identical locations, depths, occurrence times, and $M_S \leq 3.0$ magnitudes. Hence, we removed contaminated data from the catalogue but the elimination of these data did not significantly change our results. Thus, a catalogue with a threshold magnitude of 3.0 can avoid the disturbance due to quarry blasts. Since the completeness magnitude is 3.0 for this region, the earthquakes over the completeness magnitude, $M_D \geq 3.0$, are also given in the same figure. In addition, the details of earthquakes with $M_D \geq 5.5$ between 1970 and 2009 are given in Table 2. There are 49 earthquakes with magnitude $M_D \geq 5.0$ and so we only put 13 strong earthquakes with magnitude equal and over 5.5 and their extent of damage in Table 2.

3. TECTONICS OF THE STUDY REGION

The East Anatolian Fault Zone (EAFZ) is a 550 km long, approximately northeast-trending, sinistral strike-slip fault zone that comprises a series of faults arranged parallel, subparallel or obliquely to the general trend. The fault zone is a transform fault forming parts of boundaries between the Anatolian and the Eurasian plates, and between the Arabian and African plates (Westaway 1994).

It is considered as a conjugate structure to the North Anatolian Fault Zone (NAFZ). The EAFZ extends from Karlıova in the northeast to Kahramanmaraş area in the southwest, where it meets and forms triple junctions with the NAFZ and the Dead Sea Fault Zone (DSFZ), respectively (Bozkurt 2001).

The Dead Sea Transform Fault Zone (DSTFZ) is a 1000 km long, approximately N-S trending, sinistral intraplate strike-slip fault zone. In terms of plate tectonics, DSFZ is considered to be plate boundary of transform type, separating the African Plate to the west and Arabian Plate to the east (Şengör and Yılmaz 1981). The Arabian Plate is moving northward faster than the African Plate. This differential movement between the plates is taken up by DSFZ. From the tectonic point of view, the DSFZ joins the divergent plate boundary along the Red Sea with the zone of plate convergence along the Alpine–Himalayan belt in southern Turkey (Hempton 1987). The EAFZ and the DSFZ meet at a triple junction between the Arabian, African and Anatolian plates near Kahramanmaraş.

The Arabian and Eurasian plates collide along the Bitlis Thrust Zone, resulting in the uplift of mountains along the suture. The Bitlis Thrust Zone is a complex continent-continent and continent-ocean collisional boundary that lies north of fold-and-thrust belt of the Arabian platform and extends from southeastern Turkey to the Zagros Mountains in Iran (Şengör and Yılmaz 1981).

The area to the east of the Karlıova triple junction is characterized by a N-S compressional tectonic regime. Conjugate strike-slip faults of dextral and sinistral character paralleling the North and East Anatolian fault zones dominate the region (Bozkurt 2001). These structures include the Çaldıran Fault, Erciş Fault, Iğdır Fault, Malazgirt Fault, Süphan Fault, Kağızman Fault Zone, Tutak Fault Zone, and North East Anatolian Fault Zone (Fig. 1c). Although the conjugate strike-slip fault system dominates the active tectonics of eastern Anatolia, the E-W-trending basins of compressional origin form the most spectacular structures of the region as they indicate N-S convergence and shortening of the Anatolian plateau (Wong *et al*. 1978).

4. METHOD

It is necessary to eliminate the dependent events from the catalogue in order to make a quantitative analysis of seismicity rate changes since the aftershock activity generally masks temporal variations of the earthquake numbers and the related statistics. We declustered the earthquake catalogue using the Reasenberg (1985) algorithm to separate the dependent events from the independent ones. The cluster analysis algorithm "declusters" or decomposes a regional earthquake catalogue into main and secondary events (Arabasz and Hill 1996). It removes all the dependent events from each cluster, and substitutes them with a unique event, equivalent in energy to that of the whole cluster.

To detect the precursory seismic quiescence, we declustered the earthquake catalogue with the algorithm introduced by Reasenberg (1985). One should be aware of the fact that the declustering process introduces some artificial manipulations. In fact, the declustering algorithm contains some arbitrary parameters that allow the user to remove aftershocks in a smaller or larger time or space interval with respect to the main shock location. In study region in this work, there are 8768 earthquakes with magnitudes greater than or equal to 1.8. With the declustering algorithm, 1026 events were removed and 7742 events are obtained. The completeness magnitude, M_c, for region is calculated as 3.0 and the earthquakes with magnitude $M_D < 3.0$ are excluded from the catalogue. Thus, the number of earthquakes exceeding this magnitude threshold is 5779. The declustering algorithm took away 860 (about 15%) earthquakes and 44% of total earthquakes were removed from all data set. Consequently, this declustered catalogue is the final catalogue and contains 4919 earthquakes for Z-value analysis in the eastern part of Turkey. After completing the declustering processes, a more reliable, homogeneous and robust seismicity data has been obtained.

ZMAP software (Wiemer 2001) has been used by many authors to investigate seismic quiescence phenomena in recent years (*e.g.*, Wyss and Martirosyan 1998, Console *et al*. 2000, Chouliaras and Stavrakakis 2001, Wyss *et al*. 2004, Polat *et al*. 2008). The new release of ZMAP (version 6, freely available on the web page, http://www.seismo.ethz.ch/prod/software/zmap/index_EN) includes most of the routines adapted for MATLAB and used for many statistical analyses. Also, some authors such as Ambraseys (1989), Huang *et al*. (2002), and Cisternas *et al*. (2004) made seismic quiescence analysis for Turkey earthquakes using different methods.

Seismic quiescence can be recognized by the methodology introduced by Wiemer and Wyss (1994) and implemented in the ZMAP software. As detailed descriptions of this methodology have already been reported in several papers, a brief outline only is necessary here. The ZMAP technique allows the user to analyze and to obtain graphic displays of seismicity rate changes in both space and time, in selected magnitude ranges. It allows also the quantitative evaluation of the statistical significance of any rate change (quiescence), the percentage of space-time volume interested by anomalies and the conditions by which a quiescence episode can be put in relation with a main shock. By ZMAP, a continuous image of space and time rate changes in seismicity is produced creating a grid of geographical coordinates, and associating to each grid node a selected number of the nearest events. The subset of events belonging to each grid node is sampled in short time windows, so that the average number of events occurred in a time period of several consecutive samples (foreground) can be compared with that of all the remaining samples (background).

In order to identify and describe seismic activity, many techniques have been used and most of them focus on the phenomenon of seismic quiescence. Visual inspection of the epicenter distribution, the time-distance plots and some statistical methods as well are widely used by researchers (*e.g.*, Ishida and Kanamori 1977, Kanamori 1981, Taylor *et al.* 1991, Takanami *et al.* 1996). The standard normal deviate Z-test is one of these statistical methods frequently used for analyzing seismic quiescence. We applied the ZMAP method for imaging the areas exhibiting a seismic quiescence. In order to rank the significance of quiescence, we used Z-test, generating the log term average (LTA(t)) function for the statistical evaluation of the confidence level in units of standard deviations

$$Z(t) = \frac{R_{\mathrm{all}} - R_{wl}}{\sqrt{\frac{\sigma_{\mathrm{all}}^2}{n_{\mathrm{all}}} + \frac{\sigma_{wl}^2}{n_{wl}}}} ,$$

where R_{all} is the mean rate in the overall period including T_W (from t_0 to t_e), R_{wl} is the mean rate in the considered time window (from t to $t + T_W$); σ_{all} and σ_{wl} are the standard deviations in these periods, and n_{all} and n_{wl} the number of samples; t is the "current time" ($t_0 < t < t_e$). The Z-value, calculated by the equation for all times t between t_0 and t_e to T_W (Fig. 3), is statistically appropriate for estimating seismicity rate change in a time window T_W (also indicated as iwl) in contrast with background seismicity. The Z-value computed as a function of time, letting the foreground window slide along the time duration of catalogue,

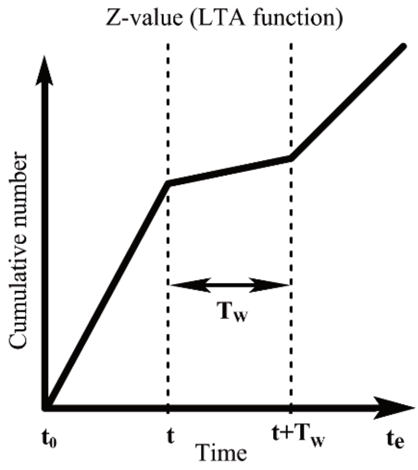

Fig. 3. Schematic explanation of how to calculate Z-value. The Z-value is calculated for all times t between t_0 and t_e to T_W , and is statistically appropriate for estimating seismicity rate change in a time window T_W in contrast with background seismicity. T_W is the length of the time window in year, and t is the "current time" ($t_0 < t < t_e$).

is called LTA(t). The shape of the LTA(t) function strongly depends on the choice of the length of the foreground window, iwl. While the statistical robustness of the LTA(t) function increases with the size of iwl, its shape becomes more and more smooth, if the iwl length exceeds the duration of the anomaly. The duration of quiescence is also an important parameter to be determined and its significance is maximized when T_W is equal to that value and for meaningful results we demand that they do not depend on the choice of T_W. Since it is not known how long quiescence may last, the window length was varied from 1.5 to 5.5 years, because this is in the range of reported seismic quiescence prior to crustal main shocks (Wyss 1997a, b).

5. RESULTS AND DISCUSSION

The cumulative number of earthquakes *versus* time for the original catalogue and for the declustered events (excluding dependent events from the original catalogue) is shown in Fig. 4a. Also, the cumulative curve for the original catalogue and for the declustered events including all events is shown in Fig. 4b. As seen in Fig. 4a, there is no significant seismicity change of reporting as a function of time between 1970 and 1995 and a little change in the seismic activity between 1995 until 2000. But further on, great seismic changes are seen in the studied area, especially after 2000. However, one can accept that the catalogue is separately homogenous from 1970 to 1995, from 1995 to 2002, and from 2002 to 2009. Since our statistical analysis is made for the earthquakes after 2000, completeness magnitude can be adopted as 3.0 for the whole catalogue after this time. The cumulative number as a function of time for eastern Turkey declustered catalogue with $M_D \geq 3.0$ has a smoother slope when compared to the clustered catalogue and it shows that the declustering has removed dependent events from the catalogue using Reasenberg's constants for California, similar to the case for the Italian earthquake catalogue as shown in Wyss *et al*. (1997). Because many stations have been constructed in this area in recent years, especially after 1999 great earthquakes in İzmit and Düzce, the other observatories, mainly KOERI, provide the real time data with the modern on-line and dial-up seismic stations in Turkey. Since this evaluation deals with the seismicity rate change and not of energy or moment release, the magnitude of completeness of the catalogue used to detect the quiescence is an important parameter because this changes regionally depending on the seismic activity of the area under investigation and the detectability of the network.

The minimum magnitude of complete recording, M_c, is an important parameter for many studies related to seismicity (*e.g.*, Taylor *et al*. 1991). It is well known that it changes with time in most catalogues, usually decreasing, because the number of seismographs increases and the methods of analysis improve. In seismicity studies, it is frequently necessary to use the maximum

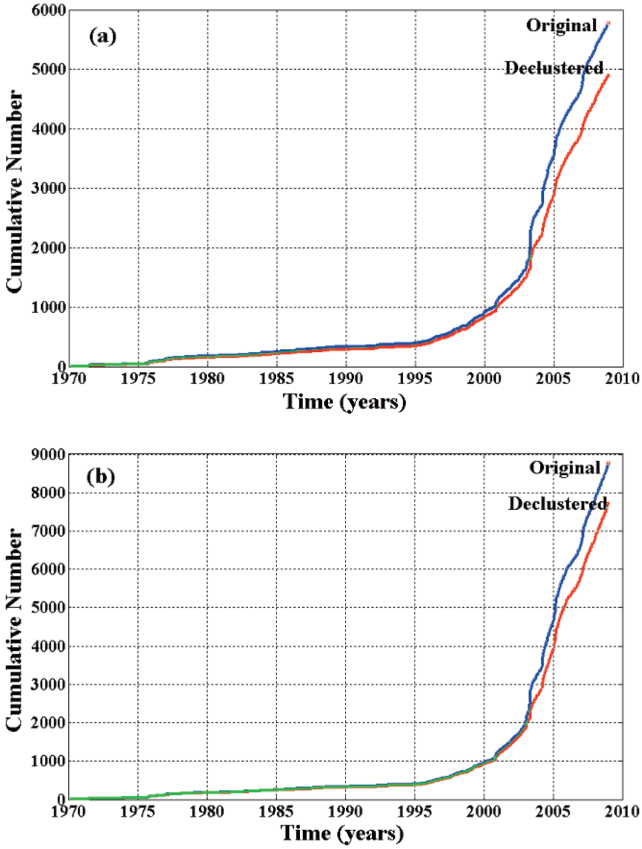

Fig. 4. Plots of cumulative number of events *versus* time: (a) for the original earthquake catalogue containing 5779 events with $M_D \geq 3.0$ (blue line) and for the declustered catalogue containing 4919 events with $M_D \geq 3.0$ (red line), (b) for the original earthquake catalogue containing 8768 events with $M_D \geq 1.8$ (blue line) and for the declustered catalogue containing 7742 events with $M_D \geq 1.8$ (red line). Each catalogue has the earthquakes with depths less than 70 km from 1970 until 2009.

number of events available for high-quality results. In order to investigate the seismic quiescence and the frequency-magnitude relationship, the change of M_c as a function of time is determined using a moving window approach with maximum curvature method (MAXC) in Woessner and Wiemer (2005). Also, M_c is calculated with entire-magnitude-range method (EMR) as stated in Woessner and Wiemer (2005). Since the result is not changed, we used MAXC method (one can find many details on the methods, in order to estimate the magnitude of completeness of earthquake catalogues, in Woessner and Wiemer 2005, Schorlemmer and Woessner 2008). We used whole earthquake catalogue containing 8768 earthquakes. Parameter M_c is estimated with its standard deviation for samples of 50 events/windows (Fig. 5a and b). It is rather large and around 4.5 between 1970 and 1995. It changes from about 4.2 to about 3.5 between 1995 and 2000. Then, it decreases to about 3.0 in the beginning of 2005 and to about 2.8 after 2005. We can easily say that it varies between 3.2 and 2.8 after 2000. The spatial distribution of M_c is also plotted at every node of 0.05º grid. As shown in Fig. 5c, it varies from 3.0 to 3.5 spatially. Magnitude completeness level is generally between 3.0 and 3.2, however it changes between 3.3 and 3.5 in some small regions. From M_c map, we clearly see that in most of the study area the seismicity resolved to $M_c = 3.0$. This result is consistent with the completeness analysis made by Huang *et al*. (2002).

The *b*-value in Gutenberg and Richter (1944) relationship is calculated by the maximum likelihood method using ZMAP software, because it yields a more robust estimate than the least-square regression method (Aki 1965). Gutenberg–

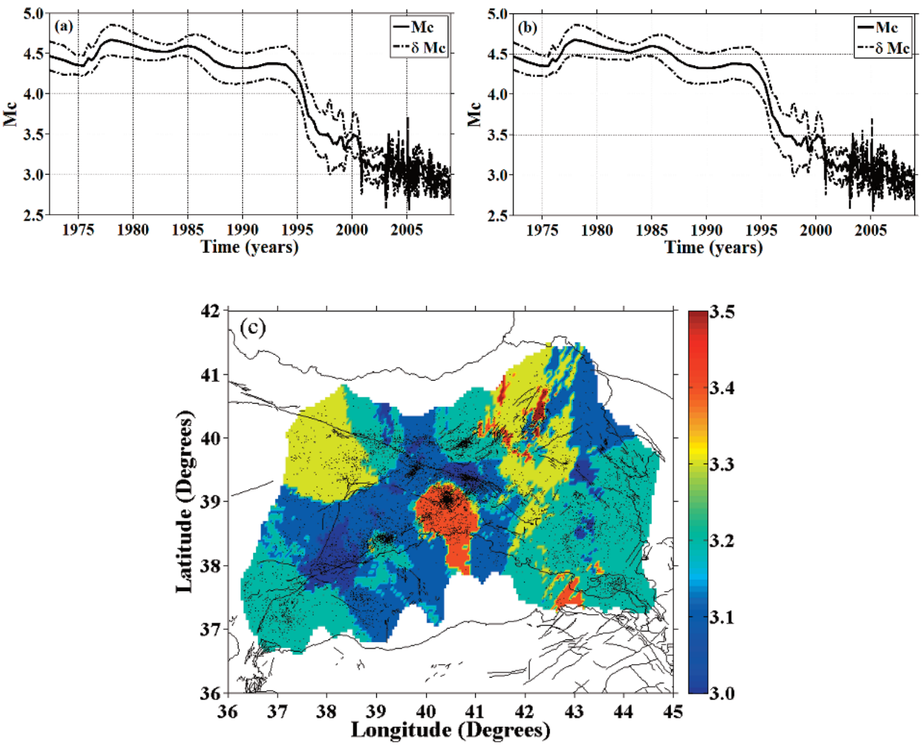

Fig. 5: (a) Magnitude of completeness, M_c, with entire-magnitude range method as a function of time; (b) M_c with magnitude curvature method as a function of time. Standard deviations (δM_c) of the M_c value are also given in both figures; (c) Geographical distribution of the M_c. Black dots show all earthquakes with $M_D \geq 1.8$.

Richter (G-R) law describes the power-law of size distribution of earthquakes. Figure 6a shows the plots of cumulative number of the earthquakes against the magnitude for study region. The completeness magnitude M_c was taken as 3.0 and using this value of completeness the *b*-value and its standard deviation is determined with the maximum likelihood method. The *b*-value is calculated as 1.07 ± 0.09. It is clearly seen that the earthquake catalogue matches the general property of events such that magnitude-frequency distribution of the earthquakes is well represented by the Gutenberg–Richter law with a *b*-value typically close to 1 (Reasenberg and Jones 1989). Also, spatial distribution of *b*-value (declustered catalogue with $M_D \geq 3.0$) for the eastern part of Turkey is presented in Fig. 6b. As in the magnitude completeness map, we considered

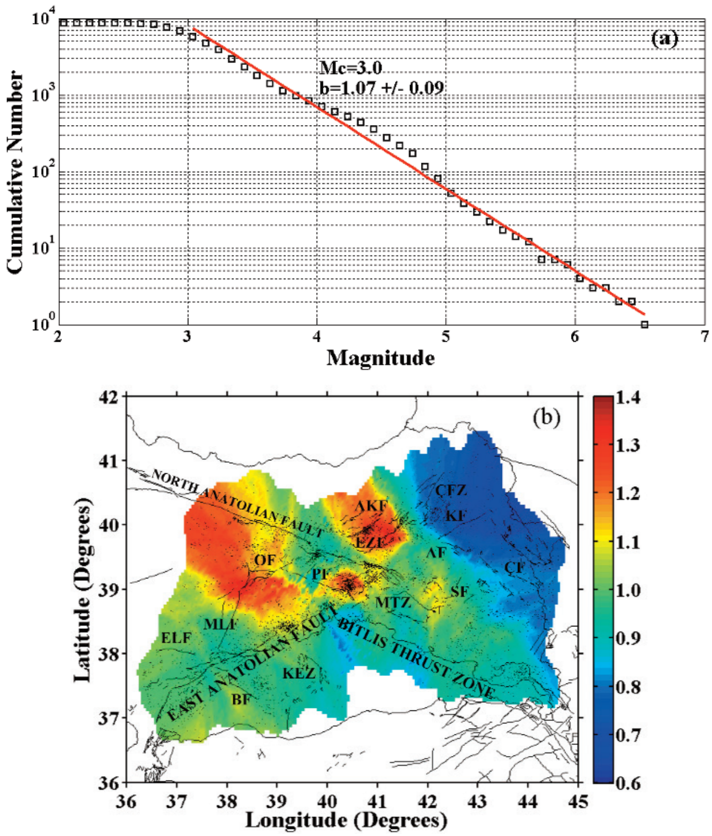

Fig. 6: (a) Frequency-magnitude distribution for the eastern part of Turkey between 1970 and 2009, the *b*-values and their standard deviation are also given; (b) Spatial distribution of the *b*-value for the study area. Black dots represent the declustered earthquakes with $M_D \geq 3.0$. Names of faults are given in caption to Fig. 1.

spatial grid of points with a grid of 0.05º. The spatial variations in *b*-value change between 0.6 and 1.4. The highest *b*-values (>1.3) are located between Bingöl and Karlıova, on Aşkale and Erzurum Faults, and in the northwest and southeast direction of Ovacık Fault. The lowest *b*-values (<0.7) are found in a large area between Çobandede Fault Zone and Başkale Fault in the direction of NW and SE.

The areas under analysis were divided into rectangular cells spacing of 0.05º in longitude and latitude because this is related to the accuracy of epicentral determinations of the catalogue and it also provides a dense coverage in space. After some preliminary tests, the nearest earthquakes $N = 50$ at each node are taken and the seismicity-rate changes are searched within a maximum radius changes by a moving time window T_W, stepping forward through the time series by a sampling interval as described by Wiemer and Wyss (1994). For each grid point we binned the earthquake population into many binning spans of 28 days for all regions in order to have a continuous and dense coverage in time. *N*- and T_W-values are usually selected accordingly in order to enhance the quiescence signal and this choice does not influence the results in anyway. The *Z*-maps based on the declustered catalogue represent a choice obtained after numerous tests, carried out trying different T_W-values (indicated as i*wl* in the respective figures) such as 1.5, 2.5, 3.5, 4.5, and 5.5 years and different starting times for the foreground windows. Regional variability of *Z*-values is presented for the beginning of 2009. Each value of *Z* is represented by a different color: the scale spans from the lowest *Z*-values, indicating no significant changes in seismicity rate, shown in blue; and the highest ones (decrease in seismicty rate), shown in grey. It should be recalled that in this representation each *Z*-value, computed in correspondence of a different grid point, comes from circular areas, the size of which is inversely proportional to the density of the spatial distribution of earthquakes. The computed *Z*-values are then contoured and mapped.

Figure 7 shows the geographical distributions of *Z*-value for different T_W-values. The length of time window for all figures is determined by adding T_W-value in years to the time chosen as the beginning of the time cut (indicated in the corresponding figures). So, all figures show the *Z*-value distribution for the same time, the beginning of 2009. As shown in Figure 7, there are four areas (A, B, C, and D) exhibiting precursory seismic quiescence. The first quiescence anomaly is found centered at 39.96ºN-40.69ºE (region A, around Aşkale, Erzurum), and the second one is found centered at 39.36ºN-39.74ºE (region B, around Ovacık, Tunceli). The third seismic quiescence is observed centered at 39.02ºN-40.52ºE (region C, including Elazığ and Bingöl), and the fourth anomaly is observed centered at 38.45ºN-42.94ºE (region D, Van Lake). Huang (2006) made a study on how to search reliable precursors is one of the key problems of the study on earthquake forecast. Huang (2006) detected a clear seismic quiescence anomaly before the 2000 western Tottori prefecture

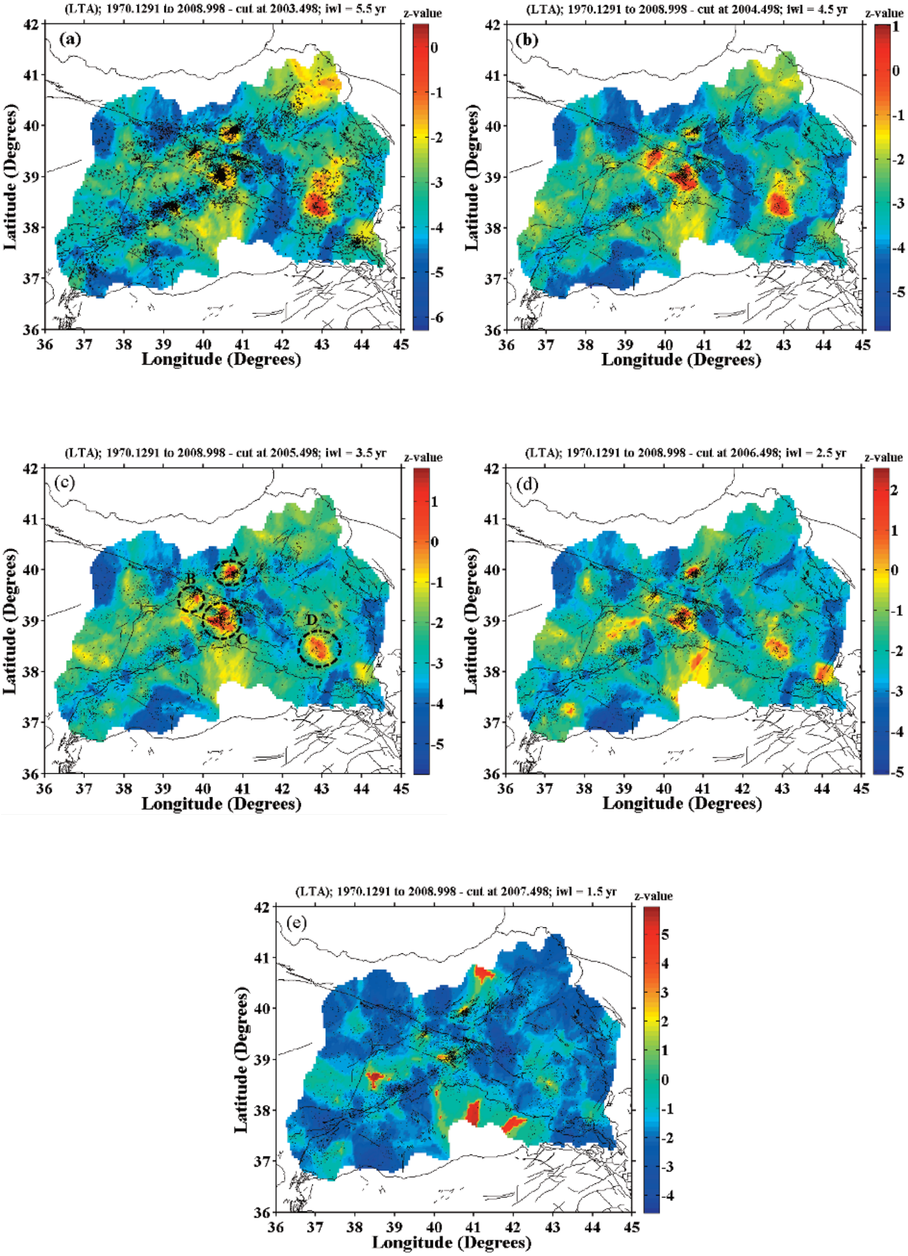

Fig. 7. Spatial distribution of Z-value for the eastern part of Turkey at the beginning of 2009 with: (a) T_W (iwl) = 5.5 years, (b) T_W (iwl) = 4.5 years, (c) T_W (iwl) = 3.5 years, (d) T_W (iwl) = 2.5 years, and (e) T_W (iwl) = 1.5 years. Black dots in panel (a) show the declustered earthquakes with $M_D \geq 3.0$ (same as in Fig. 9).

earthquake and stated that the significance or reliability of precursory seismic quiescence is an important topic for deserving further study. Thus, the above seismic quiescence anomalies for eastern Turkey should be a significant and reliable precursor and the Z-value method used in this work can enhance the reliability of precursors.

Our aim is also to identify the beginning of quiescence. To recognize these beginnings, the cumulative number of events is plotted in a circular area including detected four regions. Figure 8 shows the curves of cumulative number *versus* time and the correspondent LTA(t) function. The Z-value peaked with $Z_{max} = 1.3$ at 2005.5 for a circle of 21.56 km radius centered at region A, $Z_{max} = 1.3$ at 2005.0 for a circle of 6.31 km radius centered at region B, $Z_{max} = 1.8$ at 2004.6 for a circle of 2.53 km radius centered at region C, and $Z_{max} = 1.4$ at 2004.5 for a circle of 13.58 km radius centered at region D. We used the same starting times as 2000 and the same time windows as 3.5 years both in Z-value maps (Fig. 7) and in cumulative numbers curves (Fig. 8).

As shown in Fig. 9, spatial variability of Z-values is also presented for every six months between 2000 and 2005 by adding $T_W = 3.5$ years to the cut-off

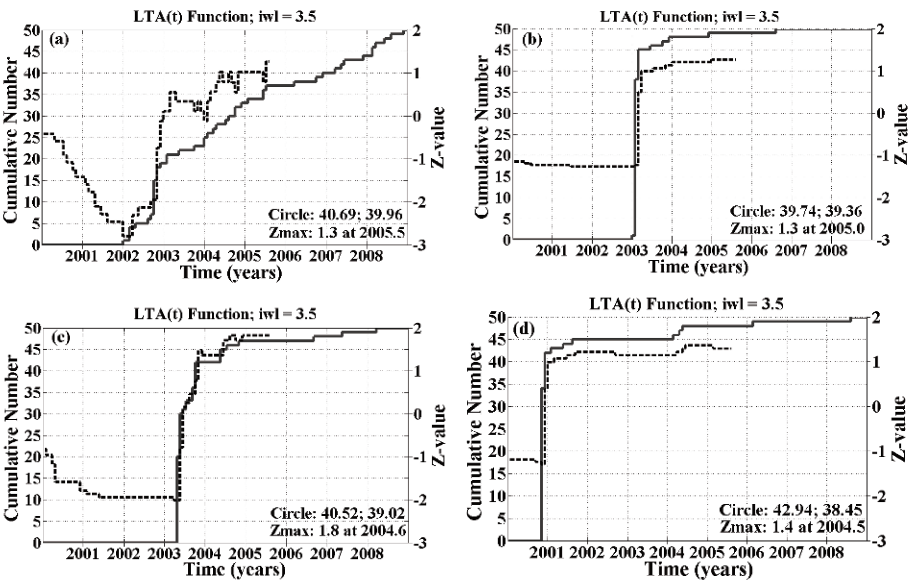

Fig. 8. Cumulative numbers of earthquakes from declustered catalogue between 2000 and 2009 (solid dark grey line) for the anomalous regions detected in Fig. 8 as a function of time with LTA(t) function (broken black line) for which the Z-value scales: (a) region A, centered at 39.96°N-40.69°E, (b) region B, centered at 39.36°N-39.74°E, (c) region C, centered at 39.02°N-40.52°E, (d) region D, centered at 38.45°N-42.94°E. Also, the center of the circles, maximum Z-values, Z_{max}, and the beginning times of the quiescence are given.

times. Our aim is to show the temporal variation of the spatial distribution of Z-values. From the observations and analysis of these maps, we can conclude that these quiescence areas are better visible for a window of 3.5 years (one can think that the map with $T_W = 4.5$ is also good). Since the quiescence anomalies found in Fig. 8 are the best revealed at the epicentral areas for $T_W = 3.5$ years

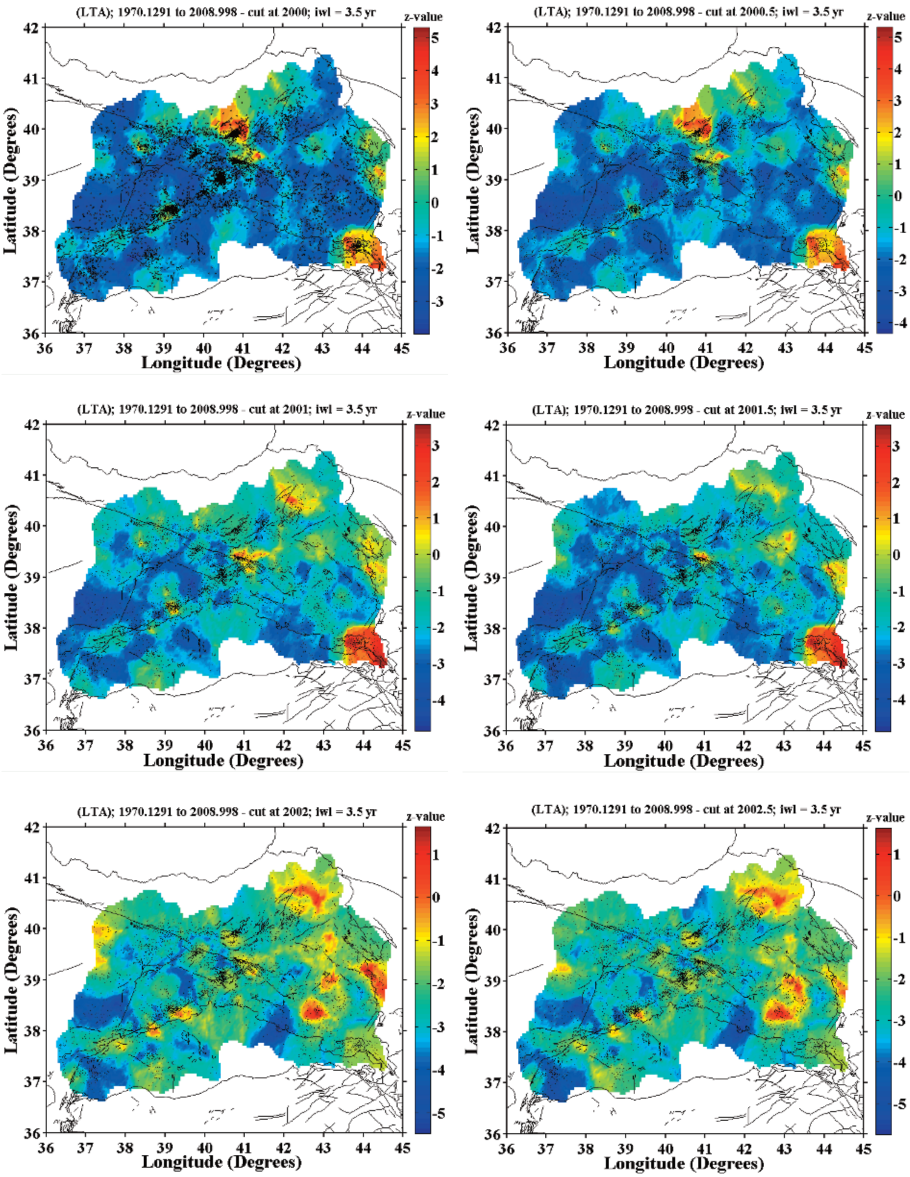

Fig. 9. Continued on next page.

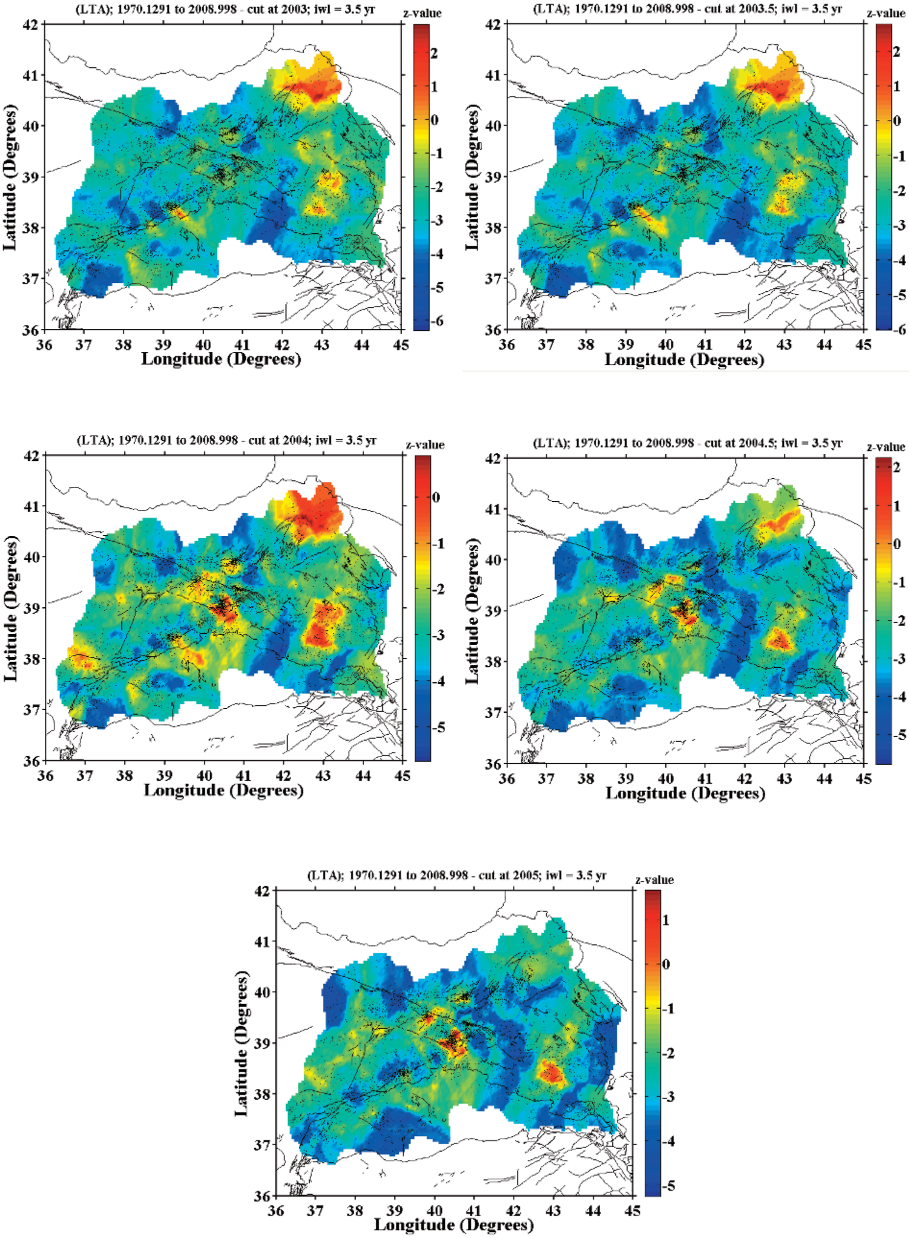

Fig. 9. Geographical distribution of Z-value for every six months between 2000 and 2005 using the declustered catalogue. The length of time window T_W (*iwl*) is selected as 3.5 years. Red color (positive Z-value) represents a decrease in seismicity rate. Black dots show the declustered earthquakes with $M_D \geq 3.0$ (same as in Fig. 7).

we used this time window length in order to image the geographical distribution of the seismicity rate changes. As shown in Z-value maps in Fig. 9, there is no significant seismic quiescence between 2001 and 2004 for the anomaly areas found in Fig. 7. In these anomaly areas, there are six earthquakes: 2000 Van, 2003 Tunceli, 2003 Bingöl, 2004 Erzurum (two earthquakes), and 2004 Elazığ earthquakes. As a result of these earthquakes, seismic activity will continue and seismic quiescence is not seen in this time period. These maps show a clear area of quiescence after 2004, especially between 2004 and 2005, nearly overlapping the centers of regions A, B, C, and D.

The temporal and spatial correlation of the quiescence may have no significance if similar quiescence anomalies occur frequently at locations in space and time where no main shocks exist (Wyss and Martirosyan 1998, Katsumata and Kasahara 1999). The alarm cube is the first attempt to visualize anomalous seismicity rate decrease in time and space in one figure. If a main shock occurs in the alarm volume, it is called a successful prediction; otherwise it is called a false alarm. The display of the high Z-values that could be false alarms is made in the alarm cubes (Wiemer 1996). Therefore, we searched for the matrix of Z-values for high Z-values, which may approach, or exceed, the Z-values recorded by the anomaly before the earthquakes. As shown in Fig. 10, in order to see all alarms and to detect the seismic quiescence not followed by a main shock, we calculated Z-value maps for all times and made alarm cube analysis using LTA(t) function (Wiemer 1996, Wyss and Martirosyan 1998). Alarms are defined as instances of Z-values larger than the selected alarm level at any node at any time. A different alarm cube can be drawn for every different Z-threshold. All values $Z \geq Z_{\mathrm{alarm}}$ as a circle at the location and time of their occurrence. We plotted the alarm cubes for a Z-threshold of 2.0, 3.0, 4.0, and 5.0 using the same parameters in the preparation of previous figures. The starts represent the location and time of occurrence of the main shocks with $M_D \geq 5.0$. In Figure 10, we showed the alarm cube comparing the seismicity rates in 3.5 years sliding rime windows to the long term mean (1970-2009). The coordinates at the bottom of the cube are the longitude and the latitude, and the vertical axis is the time progressing upward. The beginning of an alarm is marked by a circle, and the duration of it by a straight line. As shown in Fig. 10, the alarm cubes for different Z-threshold includes some outstanding groups of anomalies close to the epicenter of the main shocks. This means that some significant seismic quiescence anomalies before great earthquakes in this region were observed in the past and can be observed before the next earthquake occurrences. So, Figure 10 indicates that the results are stable according to the choice of N and T_W. The number of extension alarms increases as the threshold value decreases. So, in all alarm cubes there are many alarm groups located on/near the earthquakes with $M_D \geq 5.0$. Consequently, these alarms found alarm cubes can be considered successful characterizing quiescence of large event between 1970 and 2009.

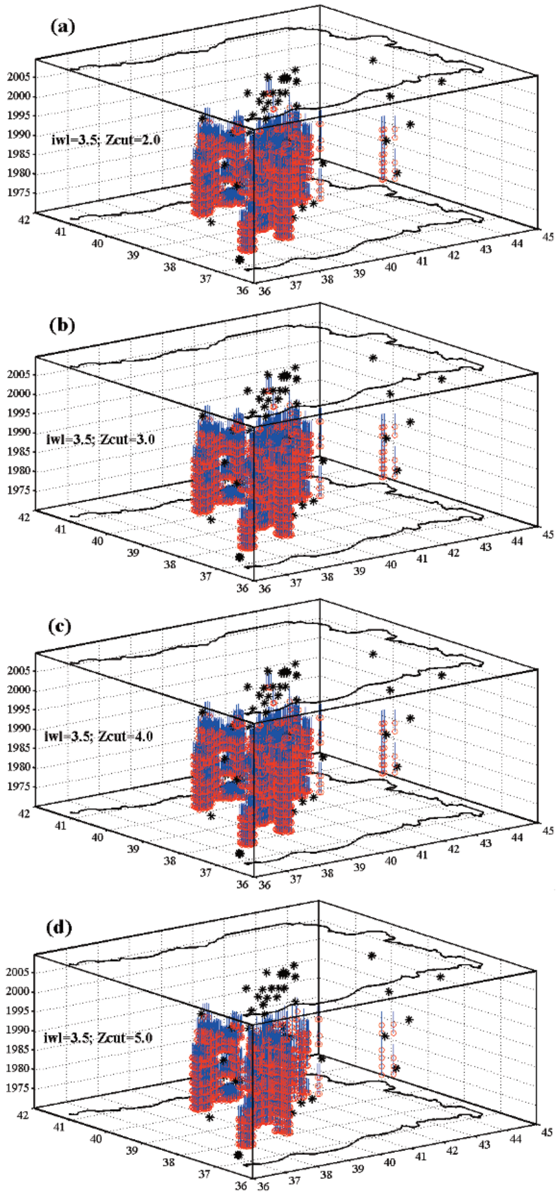

Fig. 10. Alarm cubes for the eastern part of Turkey. The start time of the alarm is represented by circles and the duration of the time window is indicated by a vertical bar. In these 3D presentations, the two horizontal axes are the latitude and longitude, the vertical axis shows time. The borders of the study area are outlined at the bottom and the top of the cube. The stars show the events with $M_D \geq 5.0$. All $Z \geq Z_{\mathrm{alarm}}$ values are shown as circles at the location and time of their occurrence.

Polat *et al*. (2008) analyzed the western part of Turkey to reveal the seismic hazard by using a number of statistical parameters such as the *b*-value in Gutenberg–Richter relationship and the seismic quiescence *Z*-value. They used LTA(*t*) function for the computation of *Z*-value and the maximum likelihood method for the calculation of *b*-value. They identified clear quiescence anomalies at several seismogenic sources. Their comparison reveals remarkable seismic hazard based on the size scaling parameters. In the same regions they found the highest *b* and *Z*-values together, whereas they found the lowest *b*-value and the highest *Z*-value. Thus, they stated that the site of lower *b*-values and higher *Z*-values has been considered to be the most likely place for a major earthquake. This could be explained with most promising environment where decrease in *b*-value is detected with an increase in mean stress (Westerhaus *et al*. 2002). Similar conclusions are also confirmed by Smith (1981) and Öncel and Wyss (2000) for the İzmit earthquake with epicenter located at the anticipated site. In this study, we observed that regions A and C have both the highest *b*- and *Z*-values. In contrast, the lower *b*-values and the higher *Z*-values are found in regions B and D. Thus, the findings and relations between *b*-value and *Z*-value in this study are quite similar with those of Polat *et al*. (2008).

Öztürk (2009) made a statistical analysis of Turkey earthquakes occurred in the eastern part of Turkey using the *Z*-value. He used the recent earthquakes with magnitude greater than 5.0 and between 36°N and 42°N in latitude and 36°E and 45°E in longitude, and in the time period between 1970 and 2005. He investigated the duration of seismic quiescence prior to the crustal main shocks that have occurred in the eastern part of Turkey and calculated the spatial variability of *Z*-values for seven different regions including 14 earthquake occurrences after 2000 because the data quality is more reliable compared to data before 2000. He used the declustered data for the calculations. In order to calculate the duration of seismic quiescence in each site for the earthquakes between 1970 and 2005, there were used three earthquakes for Van region, two earthquakes for Tunceli region, seven earthquakes for Bingöl region, four earthquakes for Malatya region, two earthquakes for Erzurum region, and two earthquakes for Elazığ region. He computed the durations of seismic quiescence as 2.87 ± 2.2 years with a significance level $Z_{max} = 2.2$ for 2000 Van earthquake, 3.27 ± 2.3 years by a significance level $Z_{max} = 2.8$ for 2003 Tunceli earthquake, 5.73 ± 0.6 years with a significance level $Z_{max} = 2.5$ for 2003 Bingöl earthquake, 3.13 ± 1.5 years with a significance level $Z_{max} = 4.8$ for 2003 Malatya earthquake, 5.04 ± 1.3 years by a significance level $Z_{max} = 4.0$ for 2004 consecutive two Erzurum earthquakes, 5.31 ± 1.2 years by a significance level $Z_{max} = 2.6$ for 2004 Elazığ earthquake, 6.07 ± 2.2 years with a significance level $Z_{max} = 1.6$ for 2005 Hakkari earthquake, 5.89 ± 0.6 years with a significance level $Z_{max} = 2.2$ for 2005 Bingöl successive five earthquakes, and 6.8 ± 1.5 years with a significance level $Z_{max} = 5.7$ for 2005 Malatya earthquake. From a statistical point of view, it is a fact that the significance of quiescence anomalies is characterized by fairly low Z-values in some earthquakes. However, some of them have a significance level Z_{max} not lower than 4.0. As shown in Fig. 10, seismic quiescence anomalies before some great earthquakes have been observed in the past and thus, the average duration of seismic quiescence before the occurrence of an earthquake in the eastern part of Turkey can be calculated as about 5.0 ± 1.5 years for the earthquakes which occurred after 2000. If we consider the fact that the beginning of quiescence is started in time between 2004.5 and 2005.5 for this study region and the duration of quiescence before the occurrence of an earthquake is identified as average 5 years for this area, it can be concluded that the regions where the significant quiescence anomalies are observed have an earthquake risk and can be interpreted as the next earthquake areas between 2009.5 and 2010.5. However, because the standard deviate of average seismic quiescence is ± 1.5 years, we can interpret that the upper limit of next earthquake occurrence may reach 2012.

Consequently, the detection of seismic quiescence is the key to the success of intermediate-term earthquake prediction. Therefore, the crustal deformation should be more carefully monitored in order to detect intermediate-term anomalies prior to a great earthquake in the near future. The last earthquake in this study region was 8 March 2010 Elazığ earthquake, which is observed in our region C. For this reason, special caution should be given to these regions in the eastern part of Turkey and monitoring of their microseismic activity by dense locally arrays, as well as the monitoring of other geophysical parameters is suggested.

6. CONCLUSIONS

A statistical assessment is made in order to map the seismic quiescence pattern for the eastern part of Turkey in the beginning of 2009 and precursory seismic quiescence from 2000 to 2009. We carried out our analysis in the rectangular area limited by the coordinates 36°N and 42°N in latitude and 36°E and 45°E in longitude. The instrumental earthquake catalogue consisting of 8768 crustal earthquakes of magnitude equal and greater than 1.8, with depths less than 70 km, are used. We used the Reasenberg algorithm in order to separate the dependent events. The number of these events in the final catalogue is reduced to 4914 with the declustering process and 44% of the earthquakes are removed. The b-value is calculated as 1.07 ± 0.09 with $M_c = 3.0$ and this value is close to 1 and typical for earthquake catalogues.

The comparison is made by means of the standard deviate Z-test generating the LTA(t) function. In order to map the spatial variability of Z-value in the beginning of 2009, we used a moving time window changing between $T_W = 1.5$ and 5.5 years and different starting times for the foreground windows.

Four areas exhibiting seismic quiescence are apparent for the eastern part of Turkey in the beginning of 2009. These anomalies are found centered at 39.96°N-40.69°E (around Aşkale, Erzurum), 39.36°N-39.74°E (around Ovacık, Tunceli), 39.02°N-40.52°E (including Elazığ and Bingöl), and 38.45°N-42.94°E (Van Lake). Spatial distribution of the seismicity rate changes is also mapped for every six months between 2000 and 2005 with $T_W = 3.5$ years. For the eastern part of Turkey, the duration of quiescence before the occurrence of an earthquake is defined as 5.0 ± 1.5 years. From this point of view, we can conclude that there is an earthquake risk in these anomaly regions where the seismic quiescences are observed and the time for a future earthquake will be exceeded between 2009.5 and 2010.5.

The last earthquake "M_W = 6.0 – Eastern Turkey, 8 March 2010, at 02:32:31 UTC" occurred where the seismic quiescence is observed in the investigated area and an outstanding seismic quiescence starting about 5 years before this main shock is observed. In this point, special attention should be given to the other anomaly regions. If such features could be recognized as a constant and reliable character of the seismicity, they could eventually contribute to the forecast of impending main shocks in future circumstances.

Acknowledgements. The authors would like to thank to Professor Stefan Weimer for providing ZMAP software and anonymous reviewers for their useful and constructive suggestions in improving this paper. We are grateful to Dr. Dogan Kalafat (KOERI) for providing us the earthquake catalogue. We also thank to KOERI for providing earthquake database via Internet.

References

Aki, K. (1965), Maximum likelihood estimate of b in the formula $\log N = a - bM$ and its confidence limits, *Bull. Earthq. Res. Inst. Tokyo Univ.* **43**, 237-239.

Ambraseys, N.N. (1989), Temporary seismic quiescence: SE Turkey, *Geophys. J. Int.* **96**, 2, 311-331, DOI: 10.1111/j.1365-246X.1989.tb04453.x.

Arabasz, W.J., and S.J. Hill (1996), Applying Reasenberg's cluster analysis algorithm to regional earthquake catalogs outside California (abstract), *Seismol. Res. Lett.* **67**, 2, 30.

Arabasz, W.J., and M. Wyss (1996), Significant precursory seismic quiescences in the extensional Wasatch front region Utah, *EOS Trans. AGU* **77**, F455.

Bayrak, Y., S. Öztürk, H. Çinar, D. Kalafat, T.M. Tsapanos, G.Ch. Koravos, and G.A. Leventakis (2009), Estimating earthquake hazard parameters from instrumental data for different regions in and around Turkey, *Eng. Geol.* **105**, 3-4, 200-210, DOI: 10.1016/j.enggeo.2009.02.004.

Bozkurt, E. (2001), Neotectonics of Turkey – a synthesis, *Geodin. Acta* **14**, 1-3, 3-30, DOI: 10.1016/S0985-3111(01)01066-X.

Chouliaras, G., and G.N. Stavrakakis (2001), Current seismic quiescence in Greece: Implications for seismic hazard, *J. Seismol.* **5**, 4, 595-608, DOI: 10.1023/A:1012025024887.

Cisternas, A., O. Polat, and L. Rivera (2004), The Marmara Sea region: Seismic behaviour in time and the likelihood of another large earthquake near Istanbul (Turkey), *J. Seismol.* **8**, 3, 427-437, DOI: 10.1023/B:JOSE.0000038451.04626.18.

Console, R., C. Montuori, and M. Murru (2000), Statistical assessment of seismicty patterns in Italy: Are they precursors of subsequent events?, *J. Seismol.* **4**, 4, 435-449, DOI: 10.1023/A:1026540018598.

Gentili, S. (2010), Distribution of seismicity before the larger earthquakes in Italy in the time interval 1994-2004, *Pure Appl. Geophys.* **167**, 8-9, 933-958, DOI: 10.1007/s00024-010-0089-x.

Gutenberg, R., and C.F. Richter (1944), Frequency of earthquakes in California, *Bull. Seismol. Soc. Am.* **34**, 185-188.

Hempton, M.R. (1987), Constraints on Arabian Plate motion and extensional history of the Red Sea, *Tectonics* **6**, 6, 687-705, DOI: 10.1029/TC006i006p00687.

Huang, Q. (2006), Search for reliable precursors: A case study of the seismic quiescence of the 2000 western Tottori prefecture earthquake, *J. Geophys. Res.* **111**, B04301, DOI: 10.1029/2005JB003982.

Huang, Q., G.A. Sobolev, and T. Nagao (2001), Characteristics of the seismic quiescence and activation patterns before the $M = 7.2$ Kobe earthquake, January 17, 1995, *Tectonophysics* **337**, 1-2, 99-116, DOI: 10.1016/S0040-1951(01)00073-7.

Huang, Q., A.O. Öncel, and G.A. Sobolev (2002), Precursory seismicity changes associated with the $M_W = 7.4$ 1999 August 17 Izmit (Turkey) earthquake, *Geophys. J. Int.* **151**, 1, 235-242, DOI: 10.1046/j.1365-246X.2002.01762.x.

Ishida, M., and H. Kanamori (1977), The spatio-temporal variation of seismicity before the 1971 San Fernando earthquake, California, *Geophys. Res. Lett.* **4**, 8, 345-346, DOI: 10.1029/GL004i008p00345.

Kanamori, H. (1981), The nature of seismicity patterns before large earthquakes. **In:** D.W. Simpson and P.G. Richards (eds.), *Earthquake Prediction. An International Review*, Maurice Ewing Series 4, American Geophysical Union, Washington DC, 1-19.

Katsumata, K., and M. Kasahara (1999), Precursory seismic quiescence before the 1994 Kurile earthquake ($M_w = 8.3$) revealed by three independent seismic catalogs, *Pure Appl. Geophys.* **155**, 2-4, 443-470, DOI: 10.1007/s000240050274.

Kumazawa, T., Y. Ogata, and S. Toda (2010), Precursory seismic anomalies and transient crustal deformation prior to the 2008 $M_w = 6.9$ Iwate-Miyagi Nairiku, Japan, earthquake, *J. Geophys. Res.* **115**, B10312, DOI: 10.1029/2010JB007567.

Mogi, K. (1969), Some features of recent seismic activity in and near Japan. 2. Activity before and after great earthquakes, *Bull. Earthq. Res. Inst. Tokyo Univ.* **47**, 395-417.

Öncel, A.O., and M. Wyss (2000), The major asperities of the 1999 $M_w = 7.4$ Izmit earthquake defined by the microseismicity of the two decades before it, *Geophys. J. Int.* **143**, 3, 501-506, DOI: 10.1046/j.1365-246X.2000.00211.x.

Öztürk, S. (2009), An application of the earthquake hazard and aftershock probability evaluation methods to Turkey earthquakes, Ph.D. Thesis, Karadeniz Technical University, Trabzon, Turkey (in Turkish with English abstract).

Öztürk, S. (2011), Characteristics of seismic activity in the Western, Central and Eastern parts of the North Anatolian Fault Zone, Turkey: Temporal and spatial analysis, *Acta Geophys.* **59**, 2, 209-238, DOI: 10.2478/s11600-010-0050-5.

Polat, O., E. Gök, and D. Yılmaz (2008), Earthquake hazard of the Aegean extension region (West Turkey), *Turkish J. Earth Sci.* **17**, 593-614.

Reasenberg, P.A. (1985), Second-order moment of central California seismicity, 1969-1982, *J. Geophys. Res.* **90**, B7, 5479-5495, DOI: 10.1029/JB090iB07p05479.

Reasenberg, P.A., and L.M. Jones (1989), Earthquake hazard after a mainshock in California, *Science* **243**, 4895, 1173-1176, DOI: 10.1126/science.243.4895.1173.

Rudolf-Navaro, A.H., A. Muñoz-Diosdado, and F. Angulo-Brown (2010), Seismic quiescence patterns as possible precursors of great earthquakes in Mexico, *Int. J. Phys. Sci.* **5**, 6, 651-670.

Rundle, J.B., W. Klein, K. Tiampo, and S. Gross (2000), Linear pattern dynamics in nonlinear threshold systems, *Phys. Rev. E* **61**, 3, 2418-2431, DOI: 10.1103/PhysRevE.61.2418.

Schorlemmer, D., and J. Woessner (2008), Probability of detecting an earthquake, *Bull. Seismol. Soc. Am.* **98**, 5, 2103-2117, DOI: 10.1785/0120070105.

Smith, W.D. (1981), The b-value as an earthquake precursor, *Nature* **289**, 136-139, DOI: 10.1038/289136a0.

Şaroğlu, F., O. Emre, and I. Kuşcu (1992), *Active Fault Map of Turkey*, General Directorate of Mineral Research and Exploration, Ankara, Turkey.

Şengör, A.M.C., and Y. Yılmaz (1981), Tethyan evolution of Turkey: A plate tectonic approach, *Tectonophysics* **75**, 3-4, 181-190, 193-199, 203-241, DOI: 10.1016/0040-1951(81)90275-4.

Takanami, T., I.S. Sacks, J.A. Snoke, Y. Motoya, and M. Ichiyanagi (1996), Seismic quiescence before the Hokkaido-Toho-Oki earthquake of October 4, 1994, *J. Phys. Earth* **44**, 3, 193-203, DOI: 10.4294/jpe1952.44.193.

Taylor, D.W.A., J.A. Snoke, I.S. Sacks, and T. Takanami (1991), Seismic quiescence before the Urakawa-Oki earthquake, *Bull. Seismol. Soc. Am.* **81**, 4, 1255-1271.

Ulusay, R., E. Tuncay, H. Sönmez, and C. Gökçeoğlu (2004), An attenuation relationship based on Turkish strong motion data and iso-acceleration map of Turkey, *Eng. Geol.* **74**, 3-4, 265-291, DOI: 10.1016/j.enggeo. 2004.04.002.

Wang, J., W. Liu, and J. Zhang (2010), Seismicity gap and seismic quiescence before 1999 Jiji (Chi-Chi) $M_W 7.6$ earthquake, *Earthq. Sci.* **23**, 4, 325-331, DOI: 10.1007/s11589-010-0729-3.

Westaway, R. (1994), Present-day kinematics of the Middle East and Eastern Mediterranean, *J. Geophys. Res.* **99**, B6, 12071-12090, DOI: 10.1029/94JB00335.

Westerhaus, M., M. Wyss, R. Yılmaz, and J. Zschau (2002), Correlating variations of b values and crustal deformations during the 1990s may have pinpointed the rupture initiation of the $M_W = 7.4$ Izmit earthquake of 1999 August 17, *Geophys. J. Int.* **148**, 1, 139-152, DOI: 10.1046/j.0956-540x.2001.01554.x.

Wiemer, S. (1996), Analysis of seismicity: new techniques and case studies, Ph.D. Thesis, University of Alaska, Fairbanks, Alaska.

Wiemer, S. (2001), A software package to analyze seismicity: ZMAP, *Seismol. Res. Lett.* **72**, 3, 373-382, DOI: 10.1785/gssrl.72.3.373.

Wiemer, S., and M. Wyss (1994), Seismic quiescence before the Landers (M = 7.5) and Big Bear (M = 6.5) 1992 earthquakes, *Bull. Seismol. Soc. Am.* **84**, 3, 900-916.

Woessner, J., and S. Wiemer (2005), Assessing the quality of earthquake catalogues: Estimating the magnitude of completeness and its uncertainty, *Bull. Seismol. Soc. Am.* **95**, 2, 684-698, DOI: 10.1785/0120040007.

Wong, H.K., E.T. Degens, and P. Finckh (1978), Structures in modern Lake Van sediments as revealed by 3.5 KHz high resolution profiling. **In:** E.T. Degens and F. Kurtman (eds.), *Geology of Lake Van*, Publ. Inst. Miner. Res. Explor. 169, 11-19.

Wyss, M. (1997a), Second round of evaluations of proposed earthquake precursors, *Pure Appl. Geophys.* **149**, 1, 3-16, DOI: 10.1007/BF00945158.

Wyss, M. (1997b), Case 23 nomination of precursory seismic quiescence as a significant precursor, *Pure Appl. Geophys.* **149**, 1, 79-113, DOI: 10.1007/BF00945162.

Wyss, M., and R.E. Habermann (1988a), Precursory seismic quiescence, *Pure Appl. Geophys.* **126**, 2-4, 319-332, DOI: 10.1007/BF00879001.

Wyss, M., and R.E. Habermann (1988b), Precursory quiescence before the August 1982 Stone Canyon, San Andreas fault, earthquakes, *Pure Appl. Geophys.* **126**, 2-4, 333-356, DOI: 10.1007/BF00879002.

Wyss, M., and A.H. Martirosyan (1998), Seismic quiescence before the M7, 1988, Spitak earthquake, Armenia, *Geophys. J. Int.* **134**, 2, 329-340, DOI: 10.1046/j.1365-246x.1998.00543.x.

Wyss, M., R. Console, and M. Murru (1997), Seismicity rate change before the Irpina (M = 6.9) 1980 earthquake, *Bull. Seismol. Soc. Am.* **87**, 2, 318-326.

Wyss, M., G.A. Sobolev, and J.D. Clippard (2004), Seismic quiescence precursors to two M7 earthquakes on Sakhalin Island, measured by two methods, *Earth Planets Space* **56**, 725-740.

Received 5 Febryary 2011
Received in revised form 27 May 2011
Accepted 2 June 2011